$4f$ and $5d$ magnetic moments in highly correlated [Ce/La/Fe] and [La/Ce/Fe] multilayers studied by x-ray magnetic circular dichroism

M. Arend
I. Physikalisches Institut, Universität Göttingen, Bunsenstrasse 9, 37073 Göttingen, Germany

M. Finazzi
European Synchrotron Radiation Facility, Boîte Postale 220, 38043 Grenoble Cedex, France

O. Schutte and M. Münzenberg
I. Physikalisches Institut, Universität Göttingen, Bunsenstrasse 9, 37073 Göttingen, Germany

A.-M. Dias, F. Baudelet, Ch. Giorgetti, and E. Dartyge
Laboratoire pour l'Utilisation du Rayonnement Electromagnétique, Bâtiment 209 D, Université Paris-Sud, 91405 Orsay, France

P. Schaaf
II. Physikalisches Institut, Universität Göttingen, Bunsenstrasse 9, 37073 Göttingen, Germany

J.-P. Kappler
Laboratoire pour l'Utilisation du Rayonnement Electromagnétique, Bâtiment 209 D, Université Paris-Sud, 91405 Orsay, France and Institut de Physique et Chimie des Matériaux de Strasbourg, 23 Rue du Loess, 67037 Strasbourg, France

G. Krill
Laboratoire pour l'Utilisation du Rayonnement Electromagnétique, Bâtiment 209 D, Université Paris-Sud, 91405 Orsay, France

W. Felsch*
I. Physikalisches Institut, Universität Göttingen, Bunsenstrasse 9, 37073 Göttingen, Germany

(Received 23 May 1997)

Experiments are reported of x-ray absorption and x-ray magnetic circular dichroism at the $L_{2,3}(2p \rightarrow 5d)$ and $M_{4,5}(3d \rightarrow 4f)$ absorption edges of Ce and La in the multilayers [La/Ce(10Å)/La/Fe(30Å)]$\times n$ and [Ce/La(10Å)/Ce/Fe(30Å)]$\times n$. In these layers, Ce adopts an α-phase-like electronic structure. Strong $3d$-$5d$ and $3d$-$4f$ hybridization is effective at the interfaces. It induces an ordered magnetic moment on the $5d$ and $4f$ states in the ground state of Ce and of the $5d$ states of La at room temperature, in antiparallel orientation to the Fe moment. By choosing the special laminar structure of the two lanthanides intercalated in between the Fe layers, the spatial extension of the Fe-induced magnetic order is directly probed. The $4f$ polarization of Ce and the $5d$ polarization of La are limited to the direct interface with Fe. In contrast, the polarization of Ce-$5d$ states extends deeply into the layers. There is evidence that the $5d$ states of α-like Ce in these layered structures are very close to a ferromagnetic instability. Remarkably, magnetic order on the Ce-$5d$ states can exist without a polarization of the $4f$ states. Apparently the $4f$-$(5d,6s)$ hybridization wins over the intraatomic $4f$-$5d$ exchange interaction, and stabilizes a nonmagnetic $4f$ ground state. Comparative studies on alloys Ce_xFe_{1-x} confirm this observation: near $x=0.34$ the polarization of the $4f$ states gets lost, but the $5d$ states are magnetically ordered. The special electronic and magnetic properties of Ce and La in the multilayer systems are reflected in the reversal of the macroscopic magnetization studied by the magneto-optical Kerr effect. [S0163-1829(98)07504-3]

I. INTRODUCTION

Magnetic ordering in ordinary rare-earth metals arises from exchange coupling between the local $4f$ moments and the conduction electrons through which the conduction band acquires a net magnetization. While this mechanism is relatively well understood for elemental rare earths, intermetallic bonding and spin-orbit coupling complicate theory in compounds of these elements with transition metals. The situation is even more complex for cerium because its $4f$-electron states are at the borderline between localization and itinerancy. Both aspects can be realized, depending on the degree of mixing of the $4f$ and conduction-electron states, either in the γ or α phases of pure Ce metal or in compounds with transition metals. Dramatic differences in the physical properties and very complex phase diagrams mirror the unlike electronic ground-state configurations.[1] Theoretical work on Ce metal has focused mostly on the transition from the fcc γ phase to the isostructural but much denser ($\approx$17%) α phase, which may be driven thermally or by the application of pressure. It has become clear by now that a good account of this transition is obtained by a model treating the $4f$-electron

states as being localized (nonbonding) in γ-Ce and itinerant (bonding) in α-Ce.[2,3] A strong hybridization of the 4f states with the conduction band makes α-Ce an archetype for a highly correlated electronic system. The interest in this element is undoubtedly linked to the fact that α-phase Ce metal itself has a nonmagnetic ground state,[4] but in compounds with d-band transition metals, like $CeFe_2$ or $CeCo_5$, where Ce adopts an α-phase-like electronic structure, experiments[5–8] and theoretical work[9–11] reveal that its ground state may be magnetically ordered, with a magnetic moment on its 4f states. An important concept in the theoretical description of the electronic structure of these compounds is the hybridization between the 3d states of the transition metal and the itinerant 4f states of Ce.

In view of these properties, experimental studies of the magnetic polarization of the electronic 4f states of Ce in highly correlated systems with magnetic d-band transition metals are of fundamental interest. This applies equally to the Ce-5d states which play a key role in the interaction between the rare earth and the transition metal tuning the magnetic properties.[12] In this context, we have recently grown multilayers combining cerium and iron, and lanthanum and iron as a non-4f reference, to probe the local electronic and magnetic properties of Ce and La near their interfaces with Fe.[13,14] These multilayers showed sharp interfaces without noticeable interdiffusion.[15] The desired information about the magnetic and electronic properties of the 4f and 5d electrons was derived by absorption spectroscopy at the $M_{4,5}$ and $L_{2,3}$ edges of Ce and La with circularly polarized x rays, taking benefit from the orbital and site selectivity of the method and the appearance of magnetic dichroism near the absorption edges involved. X-ray magnetic circular dichroism (XMCD) reflects the phenomenon that the photoabsorption cross section depends on the helicity of the incident light (left or right circularly polarized) with respect to the direction of the magnetization. The underlying mechanism, governed essentially by electric dipole transitions, implies that in the case of rare-earth elements which is of interest here photoabsorption involves the $3d \rightarrow 4f(M_{4,5})$ and $2p \rightarrow 5d(L_{2,3})$ excitation thresholds in the soft- and hard-x-ray regions, respectively. Hence the magnetic polarization of the 4f and 5d states of the rare earth can be directly and independently probed by this technique. Moreover, XMCD allows one, due to the existence of sum rules,[16,17] to separate for each edge the orbital and spin contributions to the magnetic moment in the ground state. However, it has been shown recently[18] that in the case of the 5d magnetic moment (i.e., at the $L_{2,3}$ edges) of a rare-earth element the application of these sum rules is not possible if there are both localized 4f and extended 5d states in the ground state. Fortunately, there is evidence[6,19,20] that these sum rules work correctly, in the special case of cerium, as soon as the 4f states are delocalized (i.e., hybridized with the conduction states).

The measurements of x-ray absorption performed on Ce/Fe multilayers at the Ce-$L_{2,3}$ thresholds have revealed that, on a considerable length scale near the interface with Fe, Ce adopts the electronic structure of the α phase.[13] This must be attributed to compressive strain induced on Ce by the large mismatch between the Ce and Fe layers at their interface. The corresponding XMCD spectra taken at the Ce-$L_{2,3}$ edges clearly demonstrate that these α-like Ce atoms carry an ordered magnetic moment on their 5d states, at room temperature, in antiparallel orientation to the Fe-layer magnetization. A similar magnetic polarization was found for the 5d states of La in the reference multilayer system La/Fe. The branching ratio of the integrated L_2 and L_3 XMCD signals is close to -1. This shows that in both cases the orbital contribution to the 5d magnetic moment is almost zero, i.e., $\langle L_z \rangle \approx 0$.[13] Hence the moment is essentially of pure spin origin. A recent XMCD study at the $M_{4,5}$ edges has shown that Ce has also a small 4f magnetic moment ($\leqslant 0.1 \mu_B$) in this α-like phase.[14]

This paper presents results which are intended to obtain a closer insight into the magnetic polarization of the 5d and 4f states of Ce in the strongly hybridized α-like phase, as well as the 5d states of La, and the spatial extension of this polarization near the interfaces in multilayers with Fe. This is accomplished by XMCD measurements at the $M_{4,5}$ and/or $L_{2,3}$ edges of thin ''probe layers'' of La and Ce which are inserted into the middle of the Ce and La counterpart sublayers of varying thickness. These experiments are complemented by similar x-ray-absorption and XMCD studies on thin films of (metastable) Ce_xFe_{1-x} alloys. In these systems, a variation of the Ce concentration x permits one to study systematically the evolution of the degree of hybridization between the Ce-4f and -5d states with the Fe-3d states and its bearing on the local magnetism on the Ce atoms.

II. SAMPLE PREPARATION AND CHARACTERISTICS

Multilayers composed of the structural periods [xÅCe/10ÅLa/xÅCe/30ÅFe] and [xÅLa/10ÅCe/xÅLa/30ÅFe] in which the Fe-layer thickness is constant, and the intercalated 10-Å-thick La or Ce films serve as probe layers, and alloy films Ce_xFe_{1-x} were grown by computer-controlled ion-beam sputtering in an ultrahigh vacuum chamber (base pressure $p < 5 \times 10^{-10}$ mbar). Highly pure sputtering gas Ar (6N) and target metals La, Ce (3N), and Fe (4N8) were used. For the preparation of the alloy films, an Fe plate of a size adapted to the desired concentration was mounted onto the Ce target. After preparation, the composition x of these films was determined by Rutherford backscattering spectrometry; it ranged between 0.17 and 0.35, with an uncertainty of ± 0.03. Partial pressures of reactive gases (e.g., O_2, N_2, H_2O) were below 10^{-10} mbar during the deposition process. Typical growth rates were near 1.0 Å /s for La and Ce, and 0.5 Å /s for Fe. Kapton or parylene foil coated with a 40-Å-thick Cr buffer layer were used as substrates for the x-ray-absorption experiments, to permit measurements in transmission mode, both in the hard- and soft-x-ray regimes, respectively. X-ray diffraction, magnetometry, and Mössbauer spectroscopy were performed on samples deposited on equally precoated Si(100) wafers. Because of the same buffer layer, the properties of the layered samples do not depend on the substrate. For the preparation of the multilayers, the sample holder was cooled to about 90 K by liquid nitrogen to minimize diffusion. The alloy films were deposited at room temperature. The total thickness of the multilayers and alloys was near 4000 Å in the case of the studies at the $L_{2,3}$ edges of Ce and La, and between 245 and 400 Å (with the total quantity of the rare earth amounting to an equivalent of 150 Å) in the case of the $M_{4,5}$-edge x-ray-

absorption measurements. A capping layer of Cr (typically 100 Å thick) provided protection against oxidation.

The structural quality of the interfaces between Fe and Ce or La in the multilayers was investigated by x-ray reflectometry in Θ-2Θ geometry at small angles.[15,21] To quantify interfacial roughness, the data were analyzed by employing results of the dynamical scattering theory.[22] Good fits were obtained for a rms roughness (full width at half maximum) of typically 3.5–4 Å in the case of the Ce/Fe interfaces and 2–3 Å for the La/Fe interfaces. Because of the very similar atomic form factor of Ce and La, conventional x-ray diffraction as employed here provides only limited information about the nature of the interfaces between La and Ce. But, as will be outlined below, the x-ray-absorption results in particular permit one to preclude noticeable interdiffusion or roughness at these interfaces. It can be concluded that the samples with their respective Ce or La probe layers present a well-defined layer structure with sharp composition profiles.

The structure of the individual layers and of the alloy films was determined by x-ray diffraction at large angles.[15,21] The 30-Å-thick Fe sublayers of the multilayers grow in the bcc structure of the α phase. Up to layer thicknesses of about 15 Å for La and 40 Å for Ce, the rare earths grow in an amorphous structure. This also applies, in particular, to the probe layers. Above these critical thicknesses, La and Ce grow in a fcc structure. The amorphous-to-crystalline transition advances gradually: once critical thicknesses have been reached (15 or 40 Å , respectively), the signatures of β-phase La or γ-phase Ce appear, and then grow in intensity as the layers become thicker. The Ce_xFe_{1-x} alloy films ($0.17 \leqslant x \leqslant 0.35$) are single phase and grow in an amorphous hence metastable structure, in agreement with the result reported previously[23] (crystalline solid solutions of Ce and Fe do not exist).

We have previously shown for Ce/Fe (Ref. 24) and La/Fe (Ref. 21) multilayers that ^{57}Fe Mössbauer spectroscopy provides information about the interaction between the lanthanides and iron at their interface. The experiments were extended to the samples with La and Ce probe layers. Due to the ferromagnetic nature of the layers, the Mössbauer spectra (not shown here) are magnetically split, with asymmetric absorption lines indicating the presence of inequivalent Fe sites. Data analysis was performed as previously:[21,24] the spectra were decomposed into a sextet representing the normal bcc part in the core of the Fe layers, and a probability distribution of magnetic hyperfine fields attributed to Fe affected by the interfaces (interface component).[25] The resulting hyperfine-field distributions $p(B_{hf})$ are compared in Fig. 1 for four representative examples. The following is noteworthy: (i) The contribution of the interface component to the total intensity of the spectrum corresponds to a nominal Fe-layer thickness of 8-9 Å per interface, both in Ce/La/Ce/Fe and La/Ce/La/Fe as in the nonintercalated multilayers.[21,24] This points to a magnetic ''proximity effect'' on a length scale exceeding the local thickness fluctuations, and mirrors a modification of the Fe electronic structure near the interface due to the lanthanide-iron interaction. (ii) The hyperfine-field distributions underlying the interface component of the spectrum, $p(B_{hf})$ present characteristic structures. As we argued previously,[21,24] these structures may be assigned to different parts of the interface. The region at

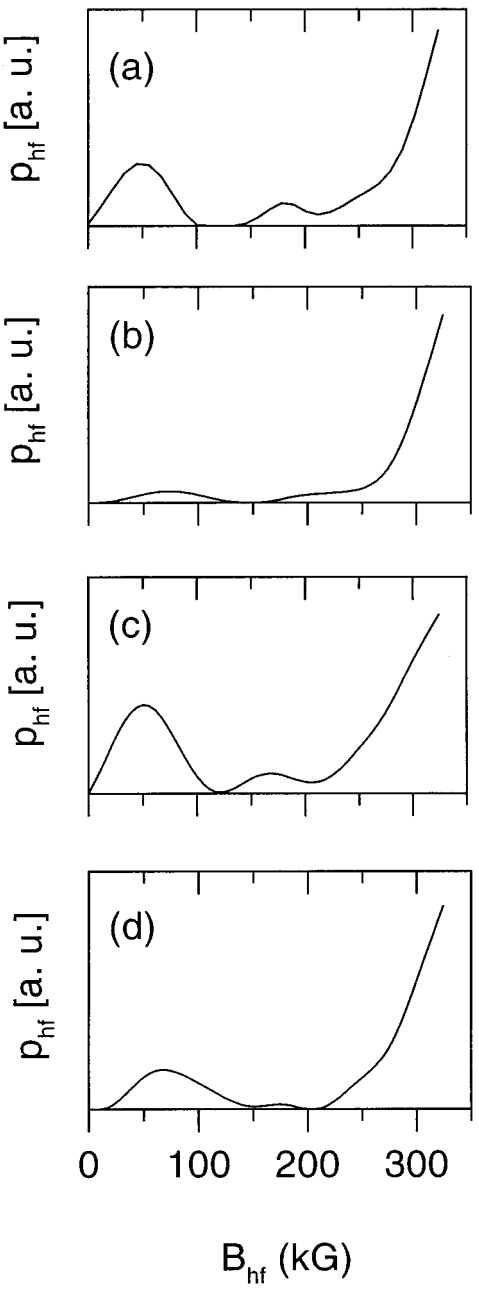

FIG. 1. Magnetic hyperfine-field distributions $p(B_{hf})$ corresponding to the contribution of the interfaces to the ^{57}Fe conversion-electron Mössbauer spectra at 300 K of the multilayers [30ÅCe/30ÅFe]×67 (a), [25ÅLa/30ÅFe]×60 (b), [10ÅCe/10ÅLa/10ÅCe/30ÅFe]×68 (c) and [10ÅLa/10ÅCe/10ÅLa/30ÅFe]×68 (d). The data in (a) and (b) are from References 24 and 21, respectively.

low fields ($B_{hf} < 150$ kG) with the distinct maximum represents Fe atoms next to the interface. For the multilayers in Fig. 1, it corresponds to 2.5 and 3 Å per interface in Ce/Fe and Ce/La/Ce/Fe, respectively, and to 1 and 2 Å per interface in La/Fe and La/Ce/La/Fe. Obviously, the maximum is more pronounced in the case where Ce sublayers are in contact with Fe. This indicates that Fe interacts differently with Ce and La at the interfaces. Note that the insertion of the Ce probe layers into the La/Fe system increases the low-B_{hf} part in the distribution $p(B_{hf})$. Interestingly, such differences ap-

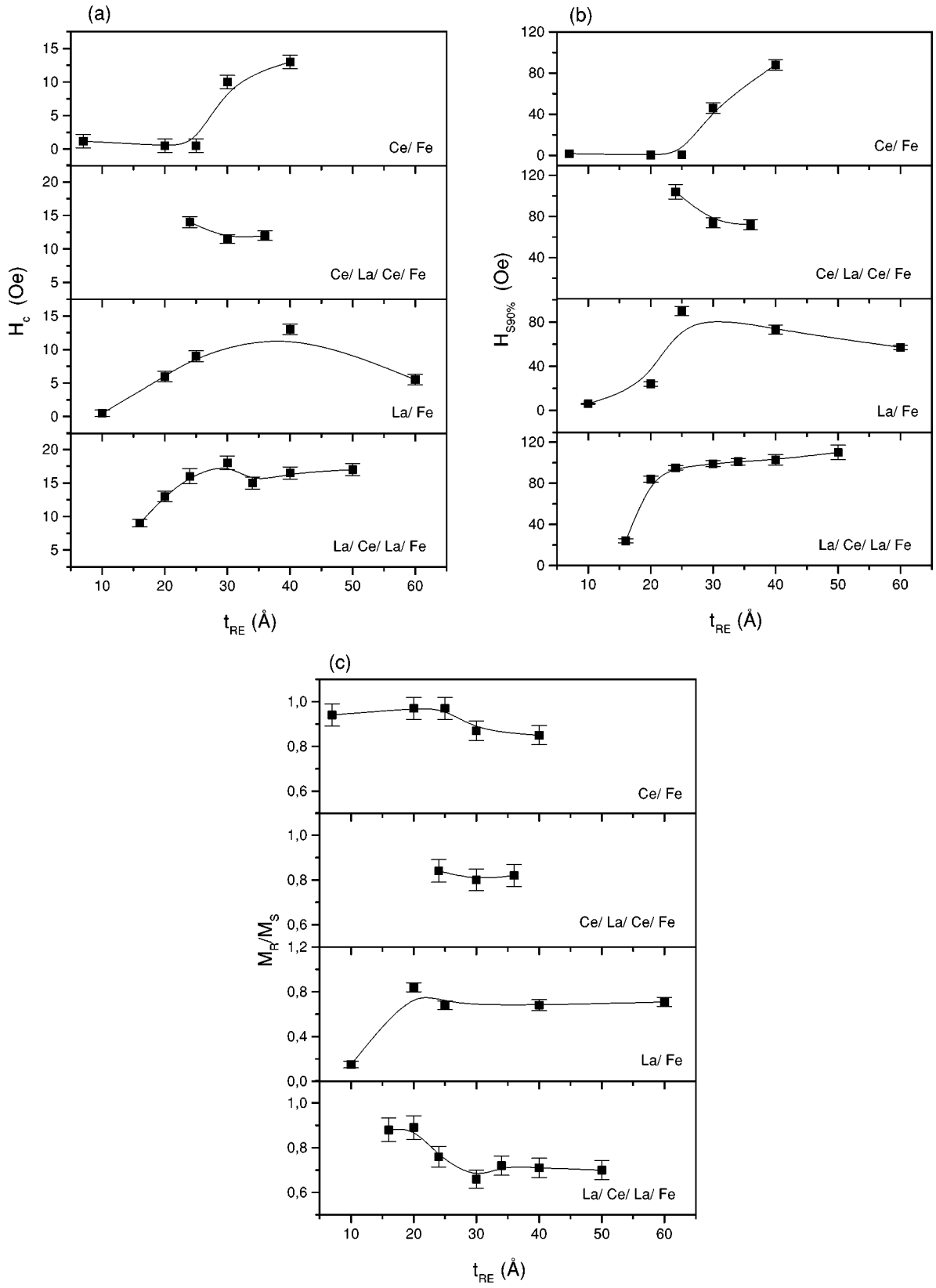

FIG. 2. Coercive fields H_C (a), fields for 90% of magnetic saturation $H_{S,90\%}$ (b), and remanent magnetizations M_R normalized with the saturation magnetization M_S (c) at 300 K determined from the longitudinal MOKE magnetization curves of the multilayers [xÅCe/30Å Fe], [xÅCe/10ÅLa/xÅCe/30ÅFe], [xÅLa/30ÅFe] and [xÅLa/10ÅCe/xÅLa/30ÅFe] vs total thickness of the rare-earth layers $t_{RE}(=t_{Ce,La}$ or $=$ [$2x$ÅLa(Ce)+10ÅCe(La)], respectively).

pear also in the values of the average magnetic hyperfine field resulting on Fe from the total ^{57}Fe Mössbauer spectra: this quantity, which is typically ≈260 kG in Ce/Fe and ≈300 kG in La/Fe, is not affected by the insertion of a 10-Å-thick La layer into the Ce, whereas it reduces to ≈285 kG following the insertion of a 10-Å-thick Ce layer into the La. (These values compare to 334 kG in bulk bcc Fe at 300 K.) We shall come back to this feature in relation with the x-ray-absorption results discussed below.

We have already shown previously[13] that the macroscopic spontaneous magnetization of the multilayers mirrors the trends observed for the average magnetic hyperfine fields. The Curie temperatures T_c of the multilayer samples are far above room temperature,[21,26] but the Ce_xFe_{1-x} alloy films order magnetically below 210 K. Both the values of T_c and of the saturation magnetization M_S agree with the results found previously for these alloys.[23] The magnetization reversal in the multilayers was studied by means of the magnetoopical Kerr effect (MOKE) in the usual longitudinal setup, with the magnetic field applied in the plane of the film and in the plane of incidence of the light beam from a He-Ne laser. Figure 2 shows the coercive field H_c, the remanence M_R, and the field for 90% of magnetic saturation, $H_{S,90\%}$, determined from the hysteresis curves of the various samples investigated. From the shape of these curves magnetic coupling of the Fe layers across the rare-earth layers can be excluded. Since the Fe-layer thickness is always the same, the observed variations of the magnetic quantities in Fig. 2 reflect the influence of the rare-earth sublayers. Indeed, they are closely related to the results from x-ray absorption (Sec. III). But the behavior is complex, and here we restrict ourselves to draw the attention to a few observations. Note that the saturation fields remain below 120 Oe and the coercive fields never exceed 18 Oe. The magnetization curves of the Ce/Fe multilayers reflect the evolution in the Ce layers from the single-phase structure (α like) at low t_{Ce} to the two-phase composite structure (α like at the interface, and γ like in the center[13]) at large t_{Ce}. The most startling feature is the very soft magnetic behavior observed at low Ce-layer thicknesses: the magnetization curves (not shown) are rectangular, with coercive and saturation fields below 1 Oe and nearly 100% remanence. On the basis of these curves it is reasonable to assume that magnetization reversal occurs essentially by the nucleation of 180° domains. Apparently the energy required is very low due to the presence of the α phase like Ce interlayers. With the appearance of γ-phase-like Ce at $t_{Ce} > 20$ Å,[13] the coercive and saturation fields H_c and $H_{S,90\%}$ increase and the remanence M_R decreases. The same magnetic hardening effect is induced by inserting a 10-Å-thick La layer into the center of the Ce layers at low t_{Ce}, where Ce is entirely α like, i.e., in Ce/La/Ce/Fe. The magnetization behavior of the La/Fe multilayers is more complex. Up to $t_{La} = 10$ Å, the material is very soft magnetically, but in contrast to the Ce/Fe system the remanence M_R is very small. This points to a domain structure in the layers. Inserting the Ce probe layer at these t_{La} values hardens the multilayers magnetically, and increases M_R drastically.

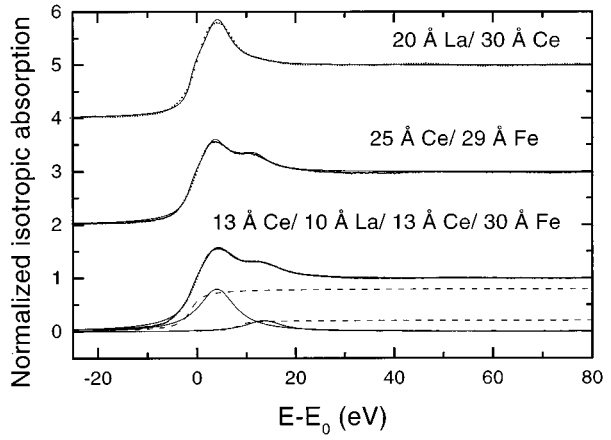

FIG. 3. Normalized x-ray-absorption spectra at the Ce-L_3 edge ($E_0 = 5723$ eV) of a Ce/La, a Ce/Fe, and a Fe/Ce/La/Ce multilayer (thickness ≈4000 Å). Thin lines: phenomenological fit. The curves were displaced vertically. At the bottom, the decomposition of a spectrum is shown by the superposition of two Lorentzians (linewidths 9 eV, thin lines) and two arctan functions (dotted lines). See text.

The x-ray absorption spectra were measured in *transmission mode* both on the energy-dispersive spectrometer D 11 of the DCI storage ring (L_2 and L_3 edges of Ce and La) and on the SU 22 beam line on the asymmetric wiggler of the Super-ACO storage ring (M_4 and M_5 edges of Ce) at LURE (Orsay, France). For the soft-x-ray experiments ($M_{4,5}$ edges) it was important to choose a weakly absorbing substrate (parylene foil, 1.5 μm thick) and to keep the multilayer and alloy films sufficiently thin in order to have about 50% of transmission, as we have indicated above. The XMCD spectra were recorded in the temperature range between 4.2 K and room temperature, in magnetic fields up to 5 kOe applied along the x-ray propagation direction, at grazing incidence (D 11) or under an angle of 60° (SU 22) with respect to the layer planes. In the latter case, some samples were measured in a field of 20 kOe. The fields are high enough to saturate the magnetization. The rate of circular polarization of the light at 0.3 mrad below the positron orbit plane is estimated to be 70% for the measurements at the $L_{2,3}$ edges, 25% at the M_5 edge, and 17% at the M_4 edge. The XMCD spectra are obtained by the difference between the absorption spectra recorded for two opposite directions of the magnetic field. Details of the data collection and the experimental setup are described elsewhere.[27,28]

III. RESULTS

A. Isotropic x-ray-absorption spectra

1. Multilayers

The ground-state electronic configuration of Ce in bulk elemental form or in systems with transition metals is reflected in the conventional x-ray-absorption spectra at its $L_{2,3}$ and $M_{4,5}$ edges which involve the dipole-allowed transitions $2p \rightarrow 5d$ and $3d \rightarrow 4f$, respectively. Since the $M_{4,5}$-edge spectroscopy is based on the transition of an electron into a $4f$ level, it probes the $4f$ configuration in the ground state obviously more directly than the $L_{2,3}$-edge spectroscopy, in

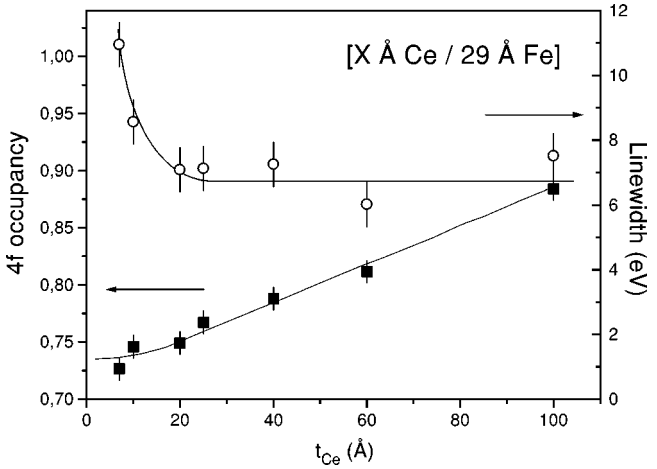

FIG. 4. Average occupation number of the Ce-4f state, n_f, and average linewidth W (resulting from the phenomenological analysis of the $L_{2,3}$ absorption edges) obtained for Ce/Fe multilayers as a function of the Ce-layer thickness t_{Ce}.

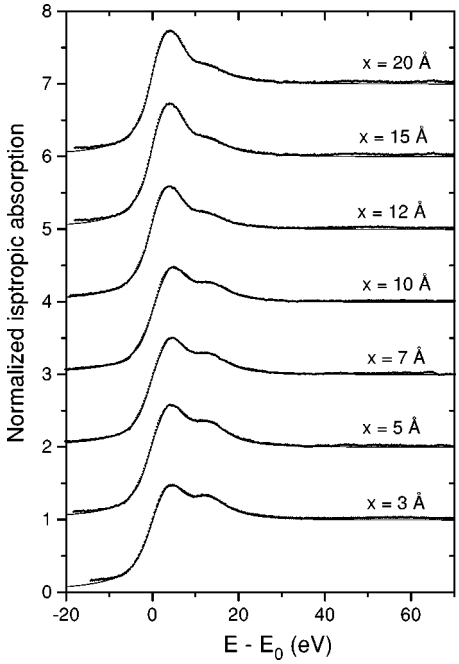

FIG. 5. Normalized x-ray-absorption spectra at the Ce-L_3 edge of the multilayers [xÅLa/10ÅCe/xÅLa/30ÅFe]$\times n$ for several La-layer thicknesses (total thickness $\approx$4000 Å). Curves are vertically displaced. Thin lines: phenomenological fit (see text).

which it is involved only indirectly as a result of final state effects.[29] Traditionally, this latter spectroscopy has been more frequently applied, and here we first focus on the study of the L_2 and L_3 edges. In Fig. 3 we display, as an example, the L_3 near-edge spectra of Ce in a Ce/La multilayer, in a Ce/Fe multilayer recently investigated,[13] and in a Ce/Fe multilayer with a La probe layer. Obviously, the replacement of La by Fe induces a profound modification of the absorption spectrum: while that of the Ce/La multilayers shows the ''white-line'' profile of the Ce-γ phase, those of the two multilayers with Fe exhibit a double-peak structure which indicates the presence of Ce with an α-phase-like electronic configuration. It should be noted that the intercalation of the La probe layer into the Ce sublayers does not visibly modify their absorption spectrum. Unfortunately, a rigorous interpretation of the measured Ce-$L_{2,3}$-edge spectra is a difficult task. In the photoabsorption process the 4f electron configuration interacts strongly with the 2p core hole. This leads to a reordering in energy of the 4f levels. As a consequence, different 4f configurations in the ground state manifest themselves as separate structures in the $L_{2,3}$-edge profiles. Hence these profiles, even though they are determined by final-state effects, are closely related to the initial 4f configuration. In a phenomenological approach,[29] widely used by experimentalists, the configuration of the electronic ground state of Ce, characterized by the ''effective occupation number of the Ce-4f states'' $n_f \leqslant 1$, is deduced from a deconvolution of the $L_{2,3}$-edge spectra: The two-line structure related to α-phase-like Ce systems is interpreted as a superposition of two white lines associated with the final states $2p^5 4f^1 5d^n$ and $2p^5 4f^0 5d^{n+1}$. The 4f ground-state occupancy n_f then is simply obtained from the relative intensities of the two white lines; their width is proportional to the width of the 5d band. It is evident that this interpretation cannot be rigorously true. More elaborate models are required to interpret the spectra. In fact, Kotani and co-workers showed[30] that a theoretical description of the Ce-$L_{2,3}$ absorption process must involve the interaction of the photoelectron and the electronic system in the final state. Malterre extended their calculations by taking into account the hybridization of the photoelectron and the conduction-band states.[31] He found that the $L_{2,3}$ near-edge spectra of Ce yield a reliable image of its ground-state configuration. Hence the phenomenological approach to the $L_{2,3}$ spectra, even if it is oversimplified, should provide a a satisfactory measure of the 4f occupancy n_f in the ground state, at least in the Ce-α phase. However, recent experiments strongly suggest that this $L_{2,3}$ spectroscopy cannot yield the correct value of n_f if n_f approaches 1.[32]

In Fig. 4 we report, for the previously investigated Ce/Fe multilayers, the variation of the *average* Ce 4f-state occupancy n_f and of the *average* linewidth W, which is correlated with the 5d-bandwidth, with the thickness of the Ce sublayers, t_{Ce}. These data were not reported explicitly in the previous paper.[13] Above $t_{Ce}=20$ Å , there is a continuous increase of n_f with increasing t_{Ce}, as well as a leveling off in W after an initial decrease. For $t_{Ce} \leqslant 20$ Å, n_f adopts the minimum value reached by α-Ce metal exposed to an external pressure;[29,33] hence Ce is in a phase with an α-like electronic configuration. As we outlined previously,[13] the observed variation of the $L_{2,3}$ absorption spectra with thickness t_{Ce} reflects the evolution in the Ce layers from this α-like phase to a two-phase structure with α-like Ce at the interfaces with Fe (up to $\approx$17 Å) and γ-like Ce in the center of the Ce layers. As stated, a possible driving mechanism for the formation of α-phase-like Ce in the multilayers is provided by stress created at the interfaces during the growth process, due to the considerable mismatch between Ce and Fe. In fact, when the mismatch is negligible at the interfaces, Ce is γ phase like as in the Ce/La multilayers (Fig. 3).

Figure 5 displays the absorption spectra near the L_3 edge of the Ce probe layer inserted into the La/Fe multilayers. The double-peak structure (which is clearly resolved even for the highest La-layer thickness $t_{La}=20$ Å) indicates that in each sample Ce is in an α-phase-like electronic configuration in

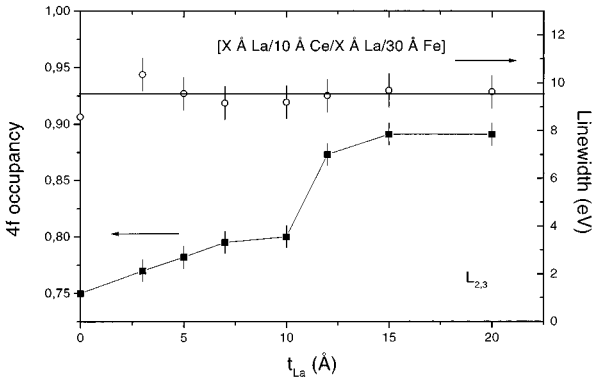

FIG. 6. Ce-4f-state occupancy n_f and average linewidth W (resulting from the phenomenological analysis of the L_3 absorption edges) in the probe layers of the multilayers [xÅLa/10ÅCe/xÅLa/30ÅFe]$\times n$ as a function of the La-layer thickness t_{La}.

these structures, presumably due to strain generated at the La/Fe interfaces. We can notice a discontinuous change in the 4f occupancy n_f for t_{La} between 10 and 12 Å . But, remarkably, the average linewidth W remains at the same high level near 10 eV (Fig. 6) in contrast to Fig. 4, where it decreases considerably with the appearance of the two-phase structure in the Ce sublayers. This reveals clearly that the electronic structure of Ce remains α like in the entire region covered by t_{La}. In contrast to the nonintercalated Ce/Fe multilayers (Fig. 4), the variation of n_f in Fig. 6 refers to *a single Ce phase* even though the overall variation nominally covers nearly the same range of values as in Fig. 4. This is not surprising since the thickness of the Ce probe layer is only 10 Å, which apparently is too low to permit the formation of a two-phase structure.

These results are corroborated by the evolution of the isotropic Ce-$M_{4,5}$ ($3d \rightarrow 4f$) absorption spectra reported in Fig. 7(a). For comparison, we also report the absorption spectrum at the M_4 and M_5 edges of La for one of the intercalated multilayers. In the case of Ce, both the M_4 and M_5 edges are characterized (mainly) by a two-peak structure which corresponds to the final states $3d^9 4f^2$ (main contribution) and $3d^9 4f^1$ (satellite contribution at the high photon-energy side). They are directly related to the initial $3d^{10}4f^1$ and $3d^{10}4f^0$ configurations, since the absorption process involves the transition into the 4f configuration. When compared to the spectrum of a typical γ-phase-like Ce system,[34] the fine structure in the M_4 and M_5 components arising from the atomic multiplets is smeared out. These features confirm the α-like character of Ce for *all* values of t_{La}. The theoretical description of the $M_{4,5}$ absorption thresholds in highly correlated Ce systems appears to be much more clear than that of the $L_{2,3}$ edges.[35,36] Thus it is possible to adjust the *experimental* n_f values, extracted from the $M_{4,5}$ spectra, in order to determine the *correct* value of n_f in the ground state. For the case of strong hybridization (4f bandwidth typically in the 2-eV range), we obtain the estimation of n_f presented in Fig. 7(b). The numbers are close to the ones resulting from the $L_{2,3}$-edge profiles (Fig. 6); in particular, the discontinuous increase at a La-layer thickness between 10 and 12 Å is reproduced.

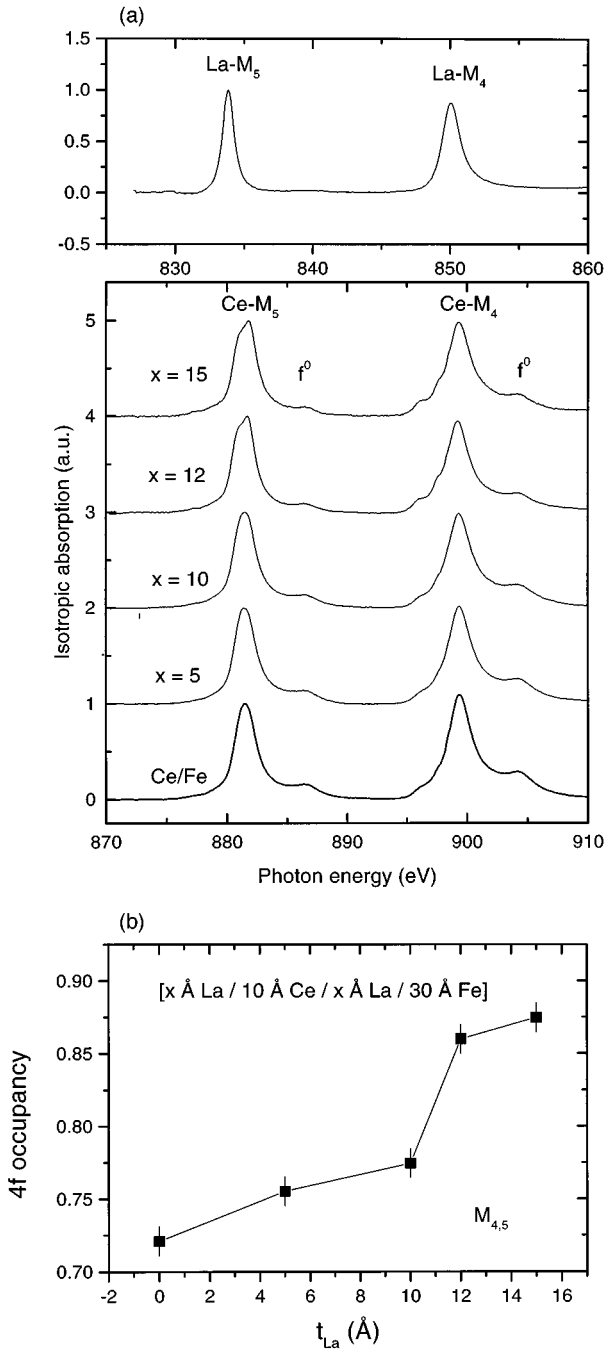

FIG. 7. (a) X-ray-absorption spectra at the Ce-$M_{4,5}$ edges of the multilayers [10ÅCe/29ÅFe]$\times$12 and [xÅLa/10ÅCe/xÅLa/30ÅFe] $\times n$ and at the La-$M_{4,5}$ edges of the multilayer [5ÅLa/10ÅCe/5Å La/30ÅFe]$\times$8 (upper curve). The spectra were arbitrarily normalized to unity at the M_5 edge; they have been vertically displaced. f^0: satellite related to the initial Ce configuration $3d^{10}4f^0$. (b) Occupation number of the Ce-4f states, n_f, deduced from the satellite peak f^0 near the Ce-M_5 edge of the spectra in (a) as described in the text.

An important conclusion we can draw from the x-ray-absorption results is that they rule out noticeable *diffusion at the interfaces between the Ce and La layers* sandwiched in the multilayer structures. In fact, alloying of La and Ce hin ders the γ-to-α-phase transition of the latter element.[37] A

simple argument for this observation derives from the difference in the atomic volumes (they are very similar for La and Ce in the γ phase, but quite dissimilar ($\approx$17% in the α phase) and the minimization of strain energy. The isotropic x-ray-absorption spectra demonstrate that in the multilayers [xÅLa/10ÅCe/xÅLa/30ÅFe]$\times n$ and [xÅCe/10ÅLa/x ÅCe/30ÅFe]$\times n$ Ce is in the α-phase-like electronic configuration. Hence a perceptible mixing of this element with La at their interfaces can be excluded. In fact, Ce-La alloy formation (and hence the appearance of γ-like Ce) would particularly affect, for instance, the absorption spectra at low La-layer thicknesses t_{La}, but there the 4f occupation on Ce, n_f, [Figs. 6 and 7(b)] is close to the minimum value reached by α-Ce metal[29,33] and the 5d bandwidth is large and constant (Fig. 6). Appreciable diffusion at the Ce-La interfaces can also be ruled out on the basis of the hyperfine-field distributions derived from the Mössbauer spectra (Fig. 1): the insertion of the probe layers essentially preserves the characteristic differences of the nonintercalated Ce/Fe and La/Fe multilayers.

2. Alloy films

The isotropic $L_{2,3}$- and $M_{4,5}$-edge absorption spectra of Ce in the alloy films $\mathrm{Ce}_x\mathrm{Fe}_{1-x}$ reveal the double-peak structure and 4f^0 satellites, respectively, which are important characteristics of an α-like electronic structure. Figure 8(a) shows that the $M_{4,5}$-edge spectra are qualitatively very similar to the multilayer spectra displayed in Fig. 7(a). The amplitude of the 4f^0 satellite decreases with increasing Ce concentration x, which signals a progressive increase of the 4f occupancy n_f [Fig. 8(b)]. As can be seen, a corresponding variation $n_f(x)$ results from the analysis of the L_2-edge absorption spectrum, even though the absolute values are somewhat higher. But the overall change is rather small; even for the alloy most concentrated in Ce, n_f is not raised significantly. However, the XMCD spectra reveal a drastic variation of the 4f magnetic moment in the ground state with the Ce concentration x (see below).

B. X-ray magnetic circular dichroism spectra

1. Multilayers

An important result of the previous investigation is that, in the Ce/Fe and La/Fe multilayers, the Ce and La atoms in the interfacial region carry an ordered magnetic moment at room temperature, which is induced by Fe.[13,14] Magnetic polarization affects the 5d states of both lanthanides, and the 4f states of Ce. For both elements, the 5d moment is a spin moment which is oriented antiparallel to the Fe moment. The *average* values of the integrated dichroic L_2 signals, normalized to the edge, are very close for Ce and La, but there is evidence that the moments are distributed differently over the thickness of the Ce or La layers in their growth direction (see below).

The magnetic polarization in these two lanthanides, near the interfaces with Fe, is probed by XMCD experiments performed on multilayers with the structural periods [xÅCe/10ÅLa/xÅCe/30ÅFe] and [xÅLa/10ÅCe/xÅLa/ 30ÅFe]. The XMCD signals were recorded both on the intercalated 10-Å-thick La or Ce probe layers and on the

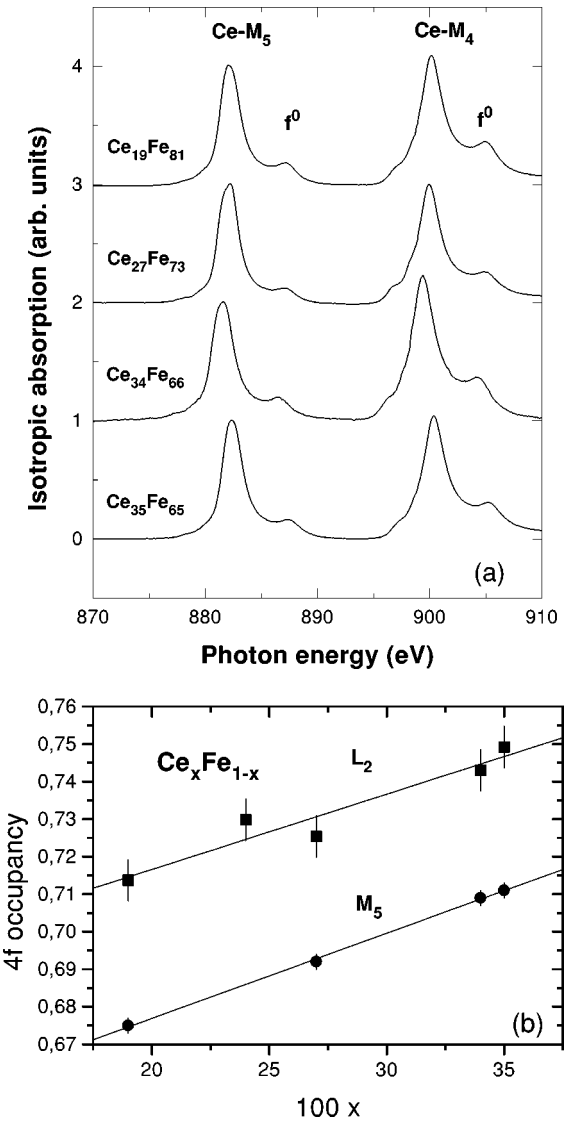

FIG. 8. (a) X-ray-absorption spectra at the Ce-$M_{4,5}$ edges of the alloy films $\mathrm{Ce}_x\mathrm{Fe}_{1-x}$. The spectra were arbitrarily normalized to unity at the M_5 edge; they have been vertically displaced. f^0: satellite related to the initial Ce configuration $3d^{10}4f^0$. (b) Occupation number of the Ce-4f states, n_f, in the alloys $\mathrm{Ce}_x\mathrm{Fe}_{1-x}$ deduced from the satellite peak f^0 near the Ce-M_5 edge of the spectra in (a) (circles) and from the analysis of the isotropic L_2-edge spectra (squares).

''spacer layers'' of varying thickness which are in direct contact with Fe. As representative examples of the spectra measured at the $L_{2,3}$ edges of the *probe-layer* elements at room temperature, we display in Figs. 9(a) and 9(b) the L_2 spectra of La, and the L_3 spectra of Ce, as well as one example of a Ce-L_2 spectrum. Obviously, the 5d states of both probe layers, La and Ce, are magnetically polarized by Fe. For Ce in La/Ce/La/Fe, the XMCD signal consists of two contributions, as the isotropic absorption signal (Fig. 5), with roughly the same splitting of $\approx$10 eV. Magnetic polarization extends considerably into the spacer layers. Figure 10 shows the variation of the integrated XMCD signal at the L_2 edge of the Ce and La probe- and spacer-layer atoms with the thickness of the spacers, t_{spacer}. Two features are noteworthy: First, *the signal on the Ce probe layer in between the La*

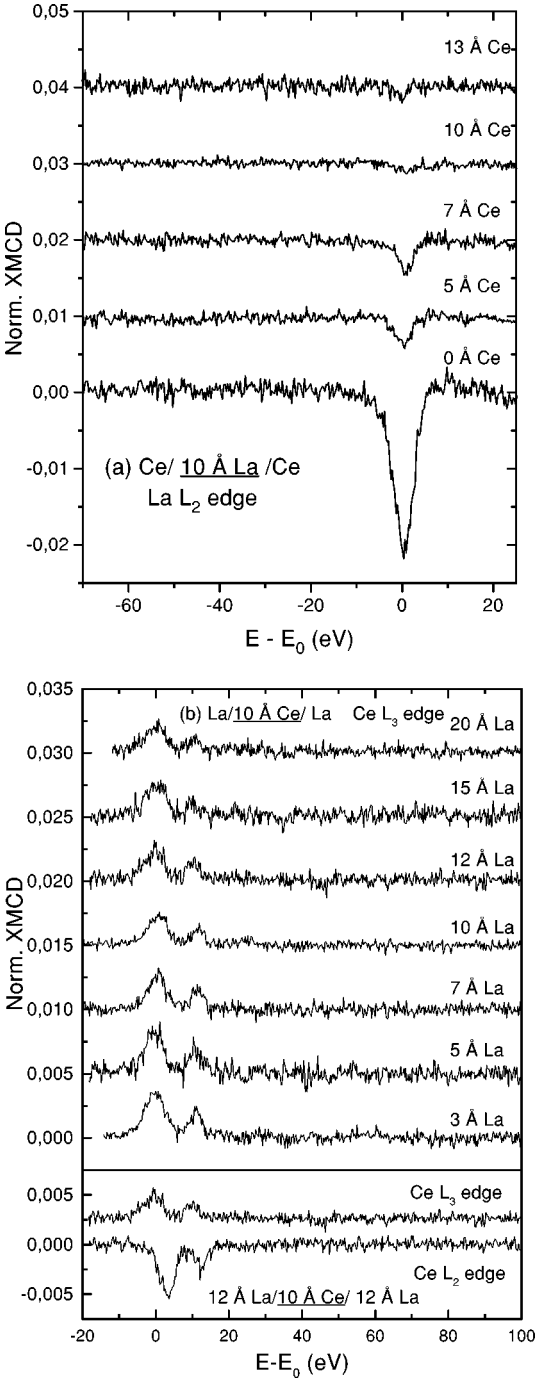

FIG. 9. Normalized XMCD spectra (a) at the La-L_2 edge (E_0 =5891 eV) in the multilayers [xÅCe/10ÅLa/xÅCe/30ÅFe]×n and (b) at the Ce-L_3 edge (E_0 = 5723 eV) in the multilayers [xÅLa/10ÅCe/xÅLa/30ÅFe]×n at room temperature. Curves vertically displaced. Lowest curve in (b): normalized Ce-L_2-edge spectrum (E_0=6164 eV) for a 12-Å-thick La spacer.

layers decays much more slowly than that on the La probe layer in between the Ce layers. This is also a strong indication that the $5d$ magnetic moment (i.e., the polarization) on the α-like Ce atoms remains important even at large distances from the Fe interfaces. Conversely, it appears that the $5d$ magnetic polarization vanishes rapidly on La with increasing distance from the interface: separating La from Fe by a 5-Å-thick Ce spacer or inserting the 10-Å-thick Ce probe layer into La reduces the signal on La dramatically.

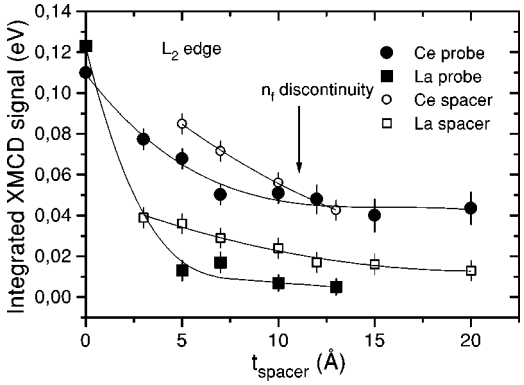

FIG. 10. Integrated normalized XMCD signal at the L_2 edge of Ce and La probe and spacer layers in the multilayers [xÅLa/10ÅCe/xÅLa/30ÅFe]×n and [xÅCe/10ÅLa/xÅCe/30ÅFe]×n as a function of the La- or Ce-layer thickness spacers measured at room temperature.

Second, *the amplitude of the XMCD signal on the α-like Ce probe layer, after an initial decrease at low distances from the interface by a factor of 2, levels off to a nearly constant value where the discontinuous change of the $4f$-state occupancy n_f occurs* (Fig. 6). However, the magnetic polarization of the $5d$ states in α-like Ce varies *continuously*, though the n_f change and the shape of the XMCD signals is not visibly modified. From the signs of the XMCD signals at the two L edges (positive for the L_3 and negative for the L_2 edge) it can be concluded that the ordered $5d$ moment is antiparallel to the Fe moment for both probe layers, as in the spacer layers and in the lanthanide layers of the pure Ce/Fe and La/Fe systems.[13] Furthermore, the branching ratio of the integrated $L_{2,3}$-edge XMCD intensities, $I(L_2)/I(L_3)$, is very close to -1 both on the probe- and spacer-layer lanthanides [see, for example, Fig. 9(b)]. This shows once more that the $4f$ electrons of Ce remain delocalized for all La-layer thicknesses, and that the sum rules[16,17] can be applied. It implies that the $5d$ orbital moment is vanishingly small in these structures, i.e., $\langle L_z \rangle = 0$. Applying the second sum rule[17] to Ce in [xÅLa/10ÅCe/xÅLa/30ÅFe] under the assumption that the magnetic dipole term $\langle T_z \rangle$ can be set to zero, we estimate the average $5d$ spin moment to be on the order of $0.13\mu_B$ for $x=0$ and of $0.06\mu_B$ for $x \geqslant 7$ Å . The absolute values of the integrated $L_{2,3}$ XMCD signals differ considerably in the spacer and probe layers in the two multilayer structures. This is emphasized in Figs. 11(a) and 11(b) where the integrated XMCD signals have been distributed, for the sake of comparison, uniformly over the individual Ce and La layers. It is obvious that this simplistic illustration of the data does not represent the real $5d$ magnetic profile in the multilayers, but it permits an immediate overview and reveals interesting features. It appears that the magnetic polarizability of the $5d$ electron states is higher in Ce than in La, Ce may be in direct contact with Fe or not. It is tempting to ''reconstruct'' the average integrated XMCD signals of the pure multilayers Ce/Fe and La/Fe by adding up the areas in Fig. 11 either on the Ce spacer layers in Ce/La/Ce/Fe and the Ce probe in La/Ce/La/Fe or on the La layers correspondingly in the other system [see Fig. 11(a)]. The resulting values are displayed in Fig. 12 as a function of the inverse rare-earth-layer thickness, together with the data for the nonintercalated

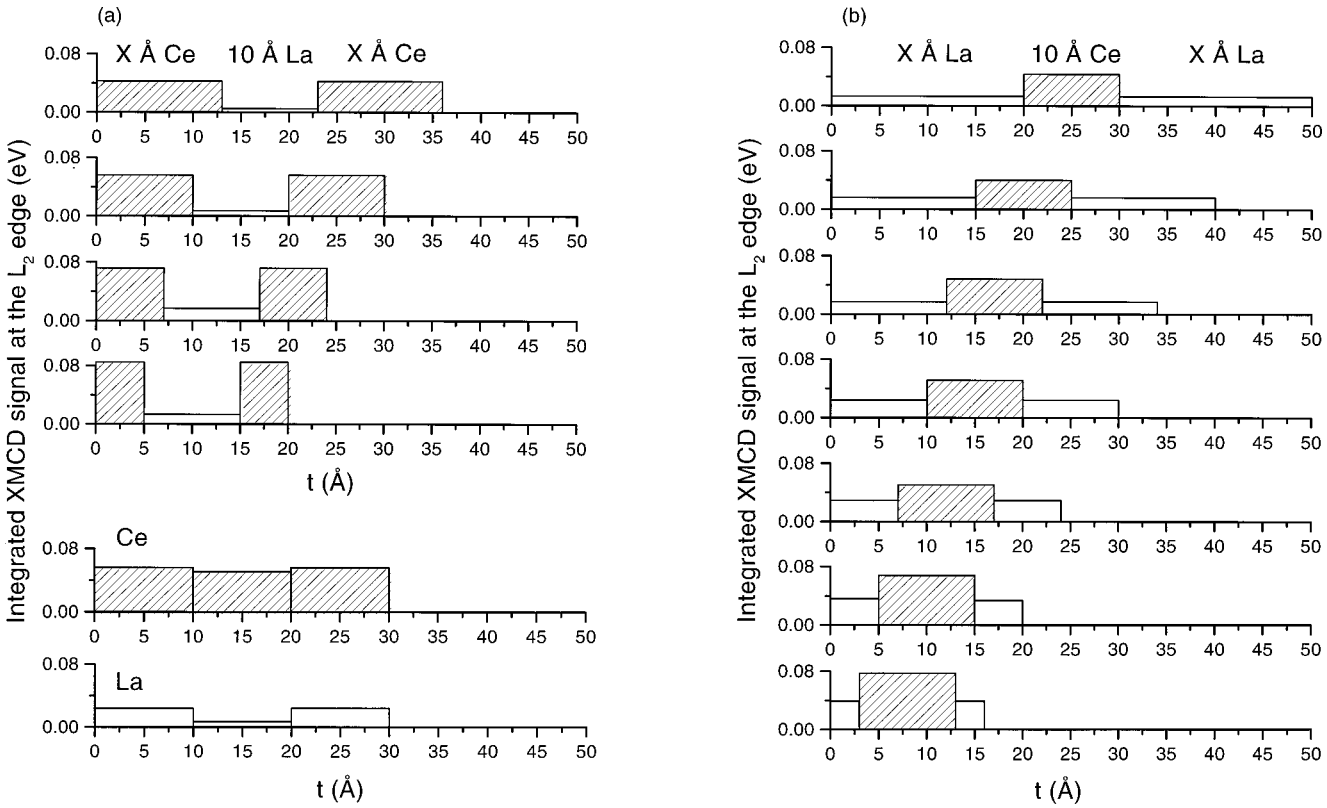

FIG. 11. Integrated normalized XMCD signals at the Ce- and La-L_2 edges at room temperature distributed uniformly over the individual rare-earth layers in the multilayers Ce/La/Ce/Fe (a) and La/Ce/La/Fe (b). Below in (a): ''reconstruction'' of the Ce and La moments as described in the text.

multilayers investigated previously.[13] These average values are very close for the pure systems. (Since in pure Ce/Fe γ-phase-like Ce develops in the center of the Ce layers when their thickness passes ≈ 20 Å which is not polarized on the 5d states,[14] we only show the data up to that thickness for this system.) In each case, the signals obey a $1/t_{\mathrm{Ce,La}}$ dependence. While the reconstructed Ce/Fe data somewhat overestimate the ones directly measured, the reconstructed La/Fe values are distinctly smaller than the ones resulting from the direct measurements. The behavior of Ce is remarkable: a 10-Å-thick Ce layer inserted into La presents almost the same Fe-induced 5d moment as if it was inserted into Ce [see Fig. 11(a), for example]. On the other hand, La behaves quite differently.

One of the most remarkable results of the present investigation is contained in Fig. 13, where the XMCD spectrum at the M_4 and M_5 edges of Ce at 77 K obtained for the multilayer [5ÅLa/10ÅCe/5ÅLa/30ÅFe]×8 is compared to that of the multilayer [10ÅCe/30ÅFe]×12 measured

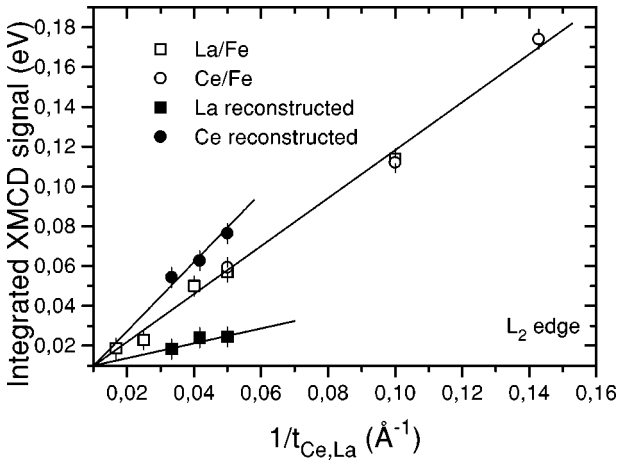

FIG. 12. Integrated normalized XMCD signal at the L_2 edge of La and Ce in the La/Fe and Ce/Fe multilayers (Fe-layer thickness 29 Å) at room temperature and reconstructed signals (see text) as a function of the inverse La- and Ce-layer thicknesses, $1/t_{\mathrm{La}}$ and $1/t_{\mathrm{Ce}}$, respectively.

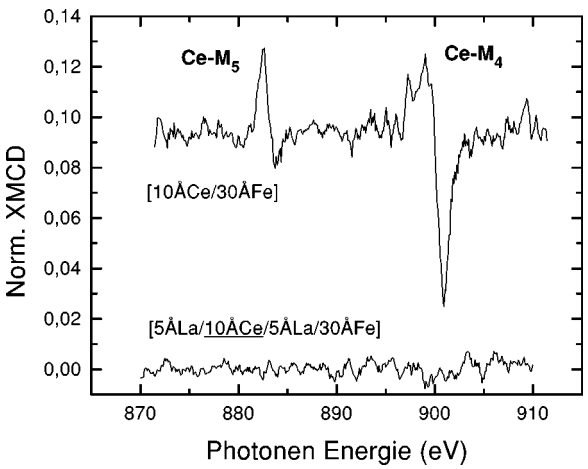

FIG. 13. XMCD spectra at the Ce-$M_{4,5}$ edges of the multilayers [10ÅCe/29ÅFe]×12 and [5ÅLa/10ÅCe/5ÅLa/30ÅFe]×8 measured at 77 K. The spectra were normalized to 100% circular polarization rate, and have been vertically displaced.

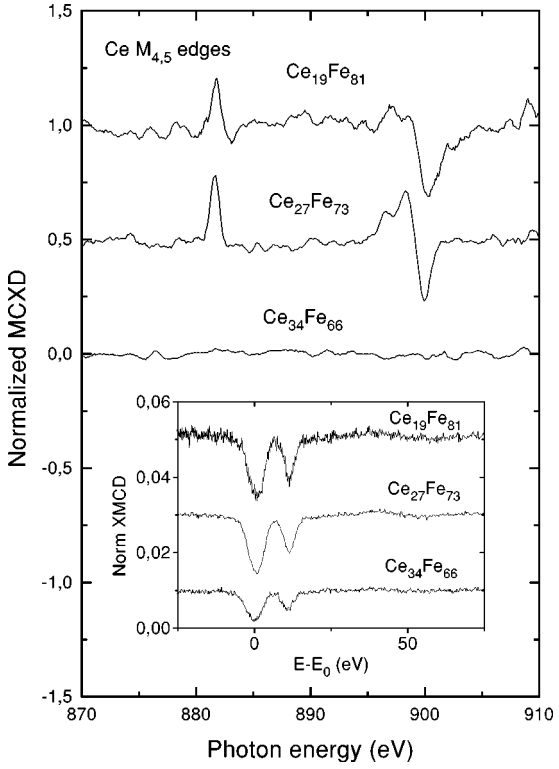

FIG. 14. XMCD spectra at the Ce-$M_{4,5}$ edges of three different alloy films Ce_xFe_{1-x} measured at 30 K. The spectra were normalized to 100% circular polarization rate and have been vertically displaced. Inset: normalized XMCD spectra at the Ce-L_2 edge measured at 11 K.

previously.[14] In both structures Ce is α like. While, obviously, the $4f$ electrons of Ce in the nonintercalated Ce/Fe multilayer (top spectrum) carry an ordered magnetic moment, a 5-Å-thick La spacer layer completely (within 0.2%) suppresses the XMCD signal on the Ce layer (bottom spectrum). Note that in contrast the XMCD amplitude at the $L_{2,3}$ edges of Ce, which probes the magnetic polarization of the $5d$ states, is only reduced by a factor of about 2 by a 5-Å-thick La spacer [compare Fig. 5 in Ref. 12 and Fig. 9(b)]. There is no doubt that a comparative reduction in the $M_{4,5}$ spectra would have to lead to an observable signal. This proves unambiguously that α-like Ce *has to be in direct contact with Fe in order to acquire a magnetic polarization of its* $4f$ *states.* In contrast, the Ce-$5d$ states are magnetically polarized across 20 Å of La [Figs. 9(b) and 10]. Thus the driving mechanism for the origin of the $4f$ moment is the direct $4f$-$3d$ hybridization and not the $4f$-$5d$ exchange interaction. This will be further addressed in Sec. IV below.

2. Alloy films

For all of the α-like Ce alloys Ce_xFe_{1-x}, XMCD spectra measured at the $L_{2,3}$ edges of Ce show the existence of an ordered $5d$ magnetic moment below the Curie temperature. These spectra (Fig. 14, inset) present the same double-peak structure as the isotropic absorption spectra, and their signs reveal again the antiparallel orientation of the Ce-$5d$ and Fe moments. We have carefully checked that the integrated XMCD signal at the L_2 edge follows the functional dependence of the macroscopic saturation magnetization on the Ce concentration and on the temperature. This implies that the dichroic signal reflects ground-state properties of the Ce ions.

The XMCD spectra at the $M_{4,5}$ edges of Ce recorded for the alloys Ce_xFe_{1-x} (Fig. 14) reveal the presence of an ordered $4f$ magnetic moment on Ce for the concentrations $x = 0.19$ and 0.27, but there is no signal (to within 0.2%, i.e., the amplitude of the noise) for $x = 0.34$, and hence no detectable $4f$ moment on Ce in this alloy. The difference between the shape of the dichroic spectra for the cases $x = 0.19$ and 0.27, respectively, reflects simply the change in the hybridization between the $4f$ and the conduction electrons. For instance, we notice the presence of the negative peak at the M_5 edge for $x = 0.19$, as in the multilayer [10 Å Ce/30 Å Fe] $\times$ 12 (Fig. 13), and the shift of the M_4 edge to lower photon energies as the Ce concentration increases from $x = 0.19$–0.27. The most remarkable result in Fig. 14 is the disappearance of the ordered $4f$ moment on Ce as x grows to 0.34 (the amplitude of the XMCD signal, if any, must be at least a factor of 10 smaller than for $x = 0.27$). Note that at this Ce concentration the alloy is still ferromagnetic, with a Curie temperature of 120 K, and the Ce-$5d$ states carry an ordered magnetic moment (Fig. 14, inset). This demonstrates again that the Fe-$3d$ states are differently effective in generating an ordered magnetic moment on the Ce-$4f$ and -$5d$ states.

IV. ON THE FE-INDUCED MAGNETIC POLARIZATION OF Ce AND La

The experimental results presented in Sec. III provide interesting information on the ground-state magnetic polarization of Ce and La in multilayers with Fe, and of Ce in Ce-Fe alloy films. They supplement the previous investigations[13,14] which have laid open the highly correlated nature of these systems. The most important aspects are the following.

(i) In the Ce/Fe multilayers, a magnetic polarization of the $5d$ states in α-phase-like Ce can exist without a magnetic polarization of the $4f$ states. $4f$ polarization requires a direct contact of the Ce and Fe atoms at the interface (Fig. 13). Similarly, in the Ce-Fe alloys, where Ce is α like, the polarization of the $4f$ states gets lost if the number of Fe neighbors becomes too small (Fig. 14).

(ii) There is a profound difference between α-like Ce and La in the multilayers with respect to the Fe-induced $5d$ magnetism. The $5d$ moment on La decreases dramatically when the material is separated from Fe by a very thin Ce spacer layer. In contrast, the $5d$ moment on α-like Ce remains important even at large distances from the Fe interfaces (Fig. 10).

It is clear that at the direct interfaces of the multilayers or locally in the alloys hybridization occurs of the $3d$ states of Fe with the itinerant $5d$ and $4f$ states of Ce and La. This induces an ordered magnetic moment on the $5d$ and $4f$ states of the lanthanides, similarly to what was discussed for the case of their compounds with the ferromagnetic transition metals by the Uppsala group.[9,11,12,38] In the multilayers one can expect, *a priori*, that the hybridization-induced magnetic polarization is of short range. Indeed the experiments show that magnetic order on the α-like Ce-$4f$ states does not extend beyond the immediate interface and must be linked to a

direct overlap of the Ce-4f and Fe-3d orbitals; it is suppressed if Ce is separated from Fe by a 5-Å-thick La layer (Fig. 13). This is related to the behavior of the alloy films Ce_xFe_{1-x}. The loss of the 4f moment on Ce between $x=0.27$ and 0.34 (Fig. 14) indicates that 4f magnetism in the ground state of an α-like Ce atom in these alloys is directly controlled by the number of Fe atoms surrounding it. Note that according to the $L_{2,3}$ XMCD spectra, 5d magnetism is less sensitive to the effects of the local environment in these alloys. Similarly to what happens in the multilayers, it survives the loss of the ordered 4f moment. Since in the compound $CeFe_2$ the Ce atoms clearly carry an ordered 4f moment,[6–9] it may be conjectured that the local Ce-Fe environment and hence the electronic structure must be distinctly different in the Laves-phase intermetallic alloy and in an amorphous alloy with the same composition. In fact, differences in the local structure are also manifest in the different mass densities[23] and in the different Curie temperatures of the two systems. For the alloy, T_c is about 100 K lower than for the compound (for $CeFe_2$, $T_c = 230$ K). The local structure of the amorphous Ce-Fe alloys was not determined in the course of our work. Unfortunately, the values of the partial coordination numbers and interatomic distances available in the literature for this material are contradictory.[39]

The magnetic polarization of the itinerant Ce-4f states in direct interface with Fe in the multilayers must be related to the pronounced maximum in the distribution of the magnetic hyperfine fields at ≈ 50 kG in the Fe sublayers of the Ce/Fe (Ref. 24) and Ce/La/Ce/Fe systems (Fig. 1). This feature is associated with the interface component of the Mössbauer spectra. In fact, it must be ascribed to the hybridization between the 3d states of Fe with the 4f states of Ce, since it is absent at the La/Fe interface. We have previously argued[24] that the effect involves Fe atoms within a ≈ 1 atomic layer at the direct interface with Ce. Magnetically, the direct interface appears as an ''alloy'' with a well-defined mean local environment. Due to the 3d-4f hybridization, it must be stabilized by strong Ce-Fe bonding, similarly as in $CeFe_2$.[9] Note that this ''interface alloy'' is magnetically ordered at room temperature (with an ordered 4f moment on the Ce-4f states and a rather low magnetic hyperfine field on the Fe sites centered around ≈ 50 kG). In contrast, the magnetic ordering temperatures of all known Ce-Fe compounds ($CeFe_2$, Ce_2Fe_{17}) and alloys are distinctly below room temperature.

5d magnetism in the multilayers appears to be much more complex than 4f magnetism, and in some features quite surprising. We first address the La/Fe system. The 5d states of La in this structure are magnetically polarized essentially at the interface only, similarly as the Ce-4f states in the Ce/Fe multilayers, by direct hybridization with the spin-split 3d states of Fe. This can be concluded from the dramatic reduction of the XMCD signal on La by only a very thin Ce spacer layer (Fig. 10). Indeed, the 5d moment of La decays rapidly with its separation from Fe. It is reduced by a factor of 10 at a distance of 5 Å only. A similar conclusion was drawn by Sève[40] from the results of x-ray resonant magnetic scattering at the L_2 edge of La in these multilayers. On the other hand, the strong reduction of the XMCD signal on La in La/Fe by the insertion of the Ce probe layer (in the structure [5ÅLa/10ÅCe/5ÅLa/30ÅFe], for example, we have a reduction by a factor of 3 [Figs. 10 and 11(b)]) must be due to a different mechanism. A plausible mechanism could be based on compressive stress on La which is generated at the interface with α-like Ce due to the considerable mismatch of the interatomic distances in the two lanthanides. The consequence is an increase of the La-5d-bandwidth, hence a decrease of the state density at the Fermi level. This translates into a reduction of the Stoner parameter and of the 5d polarization. It is clear then that the ''reconstruction'' of the average 5d moment on La from these spacer layer signals, described in Sec. III B 1, leads to a value which is too small as compared to the moment directly measured in La/Fe (Fig. 12). Moreover, the same interfacial stress in La/Ce/La/Fe may be also responsible for the Ce-induced enhancement of the hyperfine-field distribution on Fe, $p(B_{\rm hf})$, at low values of $B_{\rm hf}$ [Fig. 1(d)], and for the decrease of the average value of $B_{\rm hf}$ as compared to the nonintercalated system La/Fe. In fact here the maximum in $p(B_{\rm hf})$ at low $B_{\rm hf}$ cannot be due to hybridization between the Fe-3d and the Ce-4f states as in the binary Ce/Fe system, since the absence of an ordered 4f moment on Ce in La/Ce/La/Fe mirrors the absence of a 3d-4f hybridization.

Figure 10 shows two regimes for the magnetic polarization of the 5d states in the α-like Ce layer in La/Ce/La/Fe. These regimes are separated by the discontinuous transition in the Ce-4f-state occupancy n_f occurring at La-layer thicknesses $t_{\rm La}$ between 10 and 12 Å [Figs. 6 and 7(b)]: the integrated XMCD signal on Ce decreases progressively with increasing distance from the Fe interface up to this transition (regime I) and then remains essentially constant (regime II), whatever the value of $t_{\rm La}$ is. The XMCD signal varies continuously through the transition in n_f, and its shape is not sensitive to the actual value. It is noteworthy that this two-regime behavior in the Ce-5d polarization is reflected in the magnetization reversal in La/Ce/La/Fe as a function of $t_{\rm La}$ (Fig. 2): after an initial variation H_c, $H_{S,90\%}$, and M_R level off to an approximately constant value. The persistence of the considerable almost constant 5d-state polarization in α-like Ce at large distances from the interface with Fe in regime II is quite surprising. Note that in this regime the 5d polarization of the La spacer layers is very small. It can be excluded that this magnetic polarization on Ce is induced indirectly by the spin-split 3d states of Fe via a polarization of the (s,p) conduction electrons in the La spacer layers by a Ruderman-Kittel-Kasuya-Yosida-type mechanism. Such a mechanism would lead to a decay of the XMCD signal, together with an oscillatory variation, which is not observed. Furthermore, it would give rise to a coupling between the magnetizations of neighboring Fe layers which can be excluded by the MOKE studies. The constancy of the signal on Ce even up to a distance of 20 Å from the interface with Fe suggests strongly that magnetic order on the Ce-5d states in the layered structure is an *intrinsic property of the ground state of α-like Ce* in regime II. This intriguing hypothesis receives support from two additional observations: First, the same two-regime behavior of the XMCD signal as in Fig. 10 is observed in the La-free multilayers Ce/Fe if this signal is referred to the α-like-Ce part only.[13] Second, the integrated signal on the Ce probe layer in La/Ce/La/Fe fits almost exactly into the ''gap'' in the Ce spacer layers in the system

Ce/La/Ce/Fe if the La-layer contribution is omitted [Fig. 11(a)]. This indicates that the magnetic polarization of the Ce probe layer is not mediated by any specific property of the La spacer but is a characteristic of Ce itself, in a specific state with a $4f$-state occupation $n_f \approx 0.9$ (Fig. 6). This state is reached after a discontinuous raise of n_f near $t_{\mathrm{La}}=10$ Å, which presumably is connected with a certain strain relaxation. The electronic configuration of Ce is still α phase like (Fig. 5) but close to the transition into a γ-like phase, i.e., the $4f$ states are on the verge of localization. This can be concluded from a comparison of the n_f value in this regime and the pressure-valence phase diagram of Ce metal.[33] Min *et al.*[41] showed in a calculation that strong spin correlations exist in α-Ce. At the borderline of the transition to the γ phase, the Stoner enhancement factor is large (comparable to that of Pd), and α-Ce is very close a magnetic instability; the energy difference between the paramagnetic and ferromagnetic phases is very small. Hence it is conceivable that subtle electronic or strain effects in the multilayer environment might induce long-range magnetic order in the α-phase-like Ce sublayers. Let us recall that this applies only to the $5d$ states since magnetic order on the itinerant $4f$ states could not be detected. The observation of an α-phase-like isotropic $L_{2,3}$ and $M_{4,5}$ absorption spectrum is an indication of an important hybridization between the $4f$ and $(5d,6s)$ conduction states of Ce. Apparently, this hybridization wins over the intraatomic exchange interaction between the $4f$ and polarized $5d$ states and stabilizes a nonmagnetic $4f$ ground state. Indeed, preliminary experiments on these layered Ce-based systems have shown that the relative weight of these competing mechanisms can be reversed: Magnetic order appears on the Ce-$4f$ states due to exchange with the spin-split $5d$ states if the $4f$ hybridization is reduced and the $4f$ states become more localized.[32]

V. CONCLUSION

We have demonstrated that XMCD offers the unique possibility to study independently ordered $4f$ and $5d$ magnetism in the ground state of α-phase-like Ce in highly correlated multilayers and alloys with Fe. In the multilayers, La spacer layers intercalated between Ce and Fe reveal the profound differences between the $4f$ and $5d$ states with respect to their magnetic polarization. They enlighten also the differences for $5d$ magnetism in Ce and La. The most important result is the observation that α-phase-like Ce is very close to an instability toward intrinsic ferromagnetic order within the $5d$ states, if the $4f$-state occupation is at the borderline of the transition to the γ-like phase. Furthermore, the reversal of the macroscopic magnetization of the composite structures is closely related to the special electronic and magnetic properties of the Ce and La sublayers resulting from the isotropic and dichroic x-ray-absorption spectra. This is remarkable since the absolute values of the Fe-induced $4f$ and/or $5d$ magnetic moments are only on the order of $0.1\mu_B$.

ACKNOWLEDGMENTS

The work was supported by the Deutsche Forschungsgemeinschaft within SFB 345. M.A. benefited from a grant provided by the DAAD (Program HSP II). The authors from Göttingen are grateful for the kind hospitality of the Orsay group.

*Corresponding author. Electronic adress: wfelsch@gwdg.de

[1] See *Handbook on the Physics and Chemistry of Rare Earths*, edited by K. A. Gschneidner, Jr. and L. Eyring (North-Holland, Amsterdam, 1978), Vol. I.

[2] O. Eriksson, R. C. Albers, A. M. Boring, G. W. Fernando, Y. G. Hao, and B. R. Cooper, Phys. Rev. B **43**, 3137 (1991).

[3] B. Johansson, Philos. Mag. **30**, 469 (1974); D. Gustafson, J. McNutt, and L. O. Roellig, Phys. Rev. **183**, 435 (1969); U. Kornstädt, R. Lässer, and B. Lengeler, Phys. Rev. B **21**, 1898 (1980).

[4] D. C. Koskenmaki and K. A. Gschneidner, Jr., in *Handbook on the Physics and Chemistry of Rare Earths* (Ref. 1), p. 337.

[5] Ch. Giorgetti, S. Pizzini, E. Dartyge, A. Fontaine, F. Baudelet, C. Brouder, Ph. Bauer, G. Krill, S. Miraglia, D. Fruchard, and J.-P. Kappler, Phys. Rev. B **48**, 12 732 (1993).

[6] A. Delobbe, A.-M. Dias, M. Finazzi, J.-P. Kappler, and G. Krill (unpublished).

[7] J. P. Schillé, F. Bertran, M. Finazzi, C. Brouder, J.-P. Kappler, and G. Krill, Phys. Rev. B **50**, 2985 (1994).

[8] S. J. Kennedy, P. J. Brown, and B. R. Coles, J. Phys.: Condens. Matter **5**, 5169 (1993).

[9] O. Eriksson, L. Nordström, M. S. S. Brooks, and B. Johansson, Phys. Rev. Lett. **60**, 2523 (1988).

[10] J. Trygg, J. M. Wills, B. Johansson, and O. Eriksson, Phys. Rev. B **50**, 4200 (1994).

[11] L. Nordström, O. Eriksson, M. S. S. Brooks, and B. Johansson, Phys. Rev. B **41**, 9111 (1990).

[12] M. S. S. Brooks and B. Johansson, in *Handbook of Magnetic Materials*, edited by K. H. J. Buschow (North-Holland, Amsterdam, 1993), Vol. 7.

[13] F. Klose, O. Schulte, F. Rose, W. Felsch, S. Pizzini, C. Giorgetti, F. Baudelet, E. Dartyge, G. Krill, and A. Fontaine, Phys. Rev. B **50**, 6174 (1994).

[14] M. Finazzi, F. M. F. de Groot, A.-M. Dias, B. Kierren, F. Bertran, Ph. Sainctavit, J.-P. Kappler, O. Schulte, W. Felsch, and G. Krill, Phys. Rev. Lett. **75**, 4654 (1995).

[15] F. Klose, M. Steins, T. Kacsich, and W. Felsch, J. Appl. Phys. **74**, 1040 (1993).

[16] B. T. Thole, P. Carra, F. Sette, and G. van der Laan, Phys. Rev. Lett. **68**, 1943 (1992).

[17] P. Carra, B. T. Thole, M. Altarelli, and X. Wang, Phys. Rev. Lett. **70**, 694 (1993).

[18] F. Baudelet, Ch. Giorgetti, S. Pizzini, Ch. Brouder, E. Dartyge, A. Fontaine, J.-P. Kappler, and G. Krill, J. Electron Spectrosc. Relat. Phenom. **62**, 153 (1993); Ch. Giorgetti, Ph.D. thesis, Université Paris-Sud, 1995.

[19] M. van Veenendal, J. B. Goedkoop, and B. T. Thole, Phys. Rev. Lett. **78**, 1162 (1997).

[20] A.-M. Dias, Ph.D. thesis, Université Paris-Sud, 1997.

[21] F. Rose, O. Schulte, P. Schaaf, W. Lohstroh, and W. Felsch, Appl. Phys. A: Solids Surf. **63**, 183 (1996).

[22] L. G. Parratt, Phys. Rev. **95**, 359 (1954); L. Nevot and P. Croce, Rev. Phys. Appl. **15**, 761 (1980).

[23] K. Fukamichi, H. Komatsu, T. Goto, and H. Wakabayashi, Physica B **149**, 276 (1988).

[24] Ph. Bauer, F. Klose, O. Schulte, and W. Felsch, J. Magn. Magn. Mater. **138**, 163 (1994).
[25] J. Hesse and A. Rübartsch, J. Phys. E **7**, 526 (1974); G. LeCaer and J. M. Dubois, *ibid.* **12**, 1083 (1979).
[26] J. Thiele, F. Klose, A. Schurian, O. Schulte, W. Felsch, and O. Bremert, J. Magn. Magn. Mater. **119**, 141 (1993).
[27] F. Baudelet, E. Dartyge, A. Fontaine, C. Brouder, G. Krill, J.-P. Kappler, and M. Piecuch, Phys. Rev. B **43**, 5857 (1991); F. Baudelet, C. Brouder, E. Dartyge, A. Fontaine, J.-P. Kappler, and G. Krill, Europhys. Lett. **13**, 751 (1990).
[28] D. Lefèbvre, Ph. Sainctavit, and C. Malgrange, Rev. Sci. Instrum. **65**, 2556 (1994).
[29] J. Röhler, in *Handbook on the Physics and Chemistry of Rare Earths*, edited by K. A. Gschneidner, Jr., L. Eyring, and S. Hüfner (North-Holland, Amsterdam, 1987), Vol. 10, p. 453.
[30] T. Jo and A. Kotani, Solid State Commun. **54**, 451 (1985); A. Kotani, J. Phys. (Paris), Colloq. **48**, C9-869 (1987); A. Kotani and J. C. Parlebas, Adv. Phys. **37**, 37 (1988).
[31] D. Malterre, Phys. Rev. B **43**, 1391 (1991).
[32] M. Arend *et al.* (unpublished).
[33] J. Röhler, in *EXAFS and Near Edge Structure III*, edited by K. O. Hodgson, B. Hedman, and J. E. Penner-Hahn (Springer, Berlin, 1984), p. 679; J. Röhler, J.-P. Kappler, and G. Krill, Nucl. Instrum. Methods Phys. Res. **208**, 647 (1983).
[34] J. Ph. Schillé, F. Bertran, M. Finazzi, Ch. Brouder, J. P. Kappler, and G. Krill, Phys. Rev. B **50**, 2985 (1994).
[35] O. Gunnarsson and K. Schönhammer, in *Handbook on the Physics and Chemistry of Rare Earths*, edited by K. A. Gschneidner, Jr., L. Eyring, and S. Hüfner (North-Holland, Amsterdam, 1987), Vol. 10, p. 103.
[36] J. C. Fuggle, F. U. Hillebrecht, J.-M. Esteva, R. Karnatak, O. Gunnarsson, and K. Schönhammer, Phys. Rev. B **27**, 4637 (1983).
[37] K. A. Gschneidner, Jr. and F. W. Calderwood, in *Handbook on the Physics and Chemistry of Rare Earths*, edited by K. A. Gschneidner, Jr. and L. Eyring (North-Holland, Amsterdam, 1986), Vol. 8, Chap. 54.
[38] M. S. S. Brooks, O. Eriksson, and B. Johansson, J. Phys.: Condens. Matter **1**, 5861 (1989).
[39] M. Matsuura, T. Fukunaga, K. Fukamichi, Y. Sato, and K. Suzuki, Z. Phys. Chem. N. F. **157**, 85 (1988); M. Matsuura, K. Fukamichi, H. Komatsu, K. Aoki, T. Masumoto, and K. Suzuki, Mater. Sci. Eng. **97**, 223 (1988).
[40] L. Sève, Ph.D. thesis, Université de Grenoble, 1997.
[41] B. I. Min, H. J. F. Jansen, T. Oguchi, and A. J. Freeman, Phys. Rev. B **34**, 369 (1986).